



An activated fluorescent probe to monitor NO fluctuation in Parkinson's disease

Tao Liu^{a,1}, Xuwei Han^{a,c,1}, Xueyi Sun^a, Weijie Zhang^b, Ke Gao^{a,c}, Runan Min^{a,c}, Yuting Tian^{a,c}, Caixia Yin^{b,*}

^a Department of Chemical and Materials Engineering, Lvliang University, Lvliang 033001, China

^b Key Laboratory of Chemical Biology and Molecular Engineering of Ministry of Education, Institute of Molecular Science, Shanxi University, Taiyuan 030006, China

^c School of Chemistry and Chemical Engineering, Shanxi University, Taiyuan 030006, China

ARTICLE INFO

Article history:

Received 3 April 2024

Revised 21 June 2024

Accepted 24 June 2024

Available online 24 June 2024

Keywords:

Blood brain barrier

Nitric oxide

Fluorescent probe

Turn off/on

Parkinson's disease

ABSTRACT

The imbalance of nitric oxide (NO) homeostasis in the brain is closely related to the occurrence of Parkinson's disease (PD). Therefore, revealing the fluctuation of NO in brain is crucial for understanding the pathophysiological processes. However, currently developed NO probes are unsuitable for this purpose due to their poor blood-brain barrier permeability. Herein, a fluorescent probe (**PO-NH**) with blood-brain barrier crossing capability and high selectivity for NO was developed. Under the NO mediation, the photo-induced electron transfer (PET) process of the probe was blocked, giving an intensive fluorescence enhancement ($F/F_0 = 15$). Moreover, **PO-NH** can be used to effectively monitor changes in intracellular NO levels. Significantly, due to excellent blood-brain barrier crossing ability and near-infrared (NIR) emission, **PO-NH** is suitable for *in vivo* imaging of NO in the brain and illustrating with the deterioration of PD, the level of NO gradually increased in the brain of PD mice. We believe that **PO-NH** may provide a beneficial tool for understanding the biological function of NO in the brain and revealing the complex connection between NO and PD.

© 2025 Published by Elsevier B.V. on behalf of Chinese Chemical Society and Institute of Materia Medica, Chinese Academy of Medical Sciences.

The Parkinson's disease (PD) is one of the most common neurodegenerative diseases that affects more than 1% population over 65 years [1,2]. The characteristic manifestations of PD included resting tremor, bradykinesia, rigidity, impaired coordination and often accompanied by comorbid symptoms such as anxiety, depression, and cognitive impairment [3-5]. These symptoms seriously affect the normal life of PD patients. Therefore, the research on the pathogenesis and diagnostic medical of PD has been at the forefront of neuroscientific research [6-8].

Currently, the diagnosis of PD is mainly based on the detection of medical devices, including single-photon emission computed tomography (SPECT) [9], magnetic resonance imaging (MRI) [10], and positron emission tomography [11]. In addition, the detection of biomarkers (α-synuclein (α-syn)) in the plasma or cerebrospinal fluid was also an important means to estimate the progression of the disease [12-14]. Even so, none of these methods achieve satis-

factory specificity, sensitivity, and non-invasiveness in the diagnosis of PD.

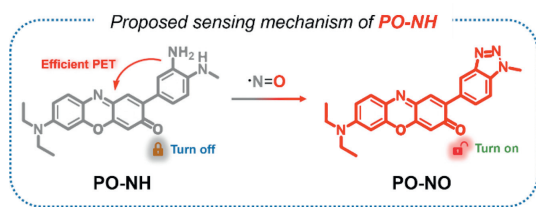
Fluorescence imaging technology using light as the medium has recently captivated a broad spectrum of attention in the chemical biology field with respect to its multitudinous excellent features, including non-invasive, high sensitivity, and real-time response [15-18]. Against the backdrop, fluorescent probes with PD biomarkers as recognition sites have been developed for the diagnosis and pathological analysis of PD [19-21].

Nitric oxide (NO) is an important neurotransmitter in the brain, and its homeostasis disorder indicates the occurrence of a variety of neurodegenerative disease [22-25]. Among them, the occurrence of PD is inextricably related to the change of nitric oxide content in the brain. Studies have shown that neuroinflammation caused by PD can cause a surge in NO levels in the brain [26]. Currently, masses of fluorescent probes have been reported to be developed to detect NO in living systems [27-30]. However, the probes used to reveal NO fluctuation in PD brain are rarely reported. A major reason may be the inadequacy of the probe's blood-brain barrier (BBB) crossing ability [31,32]. The BBB is a natural barrier that protects the brain tissue from outside substances [33,34]. There-

* Corresponding author.

E-mail address: yincx@sxu.edu.cn (C. Yin).

¹ These authors contributed equally to this work.



Scheme 1. The proposed sensing mechanism for **PO-NH** and NO.

fore, developing a probe that can monitor NO in the brain remains pretty challenging task.

Herein, we designed a NO-activated fluorescence probe **PO-NH** with near-infrared (NIR) emission. The aim is to study the complex relationship between NO and PD, and achieve *in vivo* diagnosis and evaluation of PD progression. The probe showed enhanced red emission by blocking the photo-induced electron transfer (PET) process through NO-mediated conversion of diamine into a triazole, and showed an excellent selectivity for NO (Scheme 1). Due to the small molecular structure and favorable lipophilicity of the **PO-NH** scaffold, the probe exhibits superior BBB crossing capabilities, enabling it for *in vivo* monitoring NO fluctuations in the brain. Notably, at the different pathological stages of NO was vividly revealed with **PO-NH** in PD mouse brains, which showed great potential in studying the fluctuations of NO during the pathogenesis of PD.

The synthesis of probe **PO-NH** refers to previous work [35] and the specific synthesis route is shown in Fig. S1 (Supporting information). ^1H and ^{13}C NMR spectra of all compounds are shown in Figs. S6–S10 (Supporting information).

Phenoxazine dyes have conjugate rigid plane structure and excellent electron donating properties and most of them have NIR imaging capability and good biocompatibility [36,37]. We designed and synthesized an activated fluorescent probe for specific recognition of NO based on the parent structure of phenoxazine dyes. It was mainly composed of NO recognition site (*O*-phenylenediamine structure) and parent phenoxazine dye. As shown in Fig. 1b, **PO-NH** is nonfluorescent due to PET. In the presence of NO, it emits a strong fluorescence at 660 nm, which is due to the great attenuation of its electron donating ability after the conversion of *O*-phenylenediamine into triazole, resulting in the blocking of the PET process (Scheme 1). In addition, the density functional theory (DFT) calculations (Fig. S4 in Supporting information) are also confirmed the molecular sensing mechanism. The intensity values and geometry of highest occupied molecular orbital (HOMO) and lowest unoccupied molecular orbital (LUMO) for **PO-NH** and **PO-NO** fully confirm that the probe undergoing PET process to quench the fluorescence.

The fluorescent properties of the probe **PO-NH**, were first evaluated. To our delight, it exhibits very low fluorescence quantum yield ($\varphi = 0.003$) and brightness ($\varepsilon \times \varphi = 111.6$) in phosphate buffered saline (PBS), which indicates that the fluorescence signal of **PO-NH** has the potential to be activated (Table S1 in Supporting information). In order to confirm the responsiveness of **PO-NH** to NO, we investigated its spectral properties for the detection of NO in PBS solutions. As shown in Fig. 1a, **PO-NH** essentially possessed a maximum absorption peak centered at 600 nm. After NO mediation, the absorption peak at 600 nm gradually moves to the pre-synthesized **PO-NO**, indicating that the *O*-phenylenediamine in the **PO-NH** structure was gradually transformed into triazole. Attendant to, with the increasing concentration of NO (0–100 $\mu\text{mol/L}$), there was a gradual increase about 15-fold in the emission peak at 660 nm (Fig. 1d), which indicated its favorable “off-on” ability as a NO probe. Further study on the linear fluorescence response of **PO-NH** to NO (0–80 $\mu\text{mol/L}$) show that it has a good linear re-

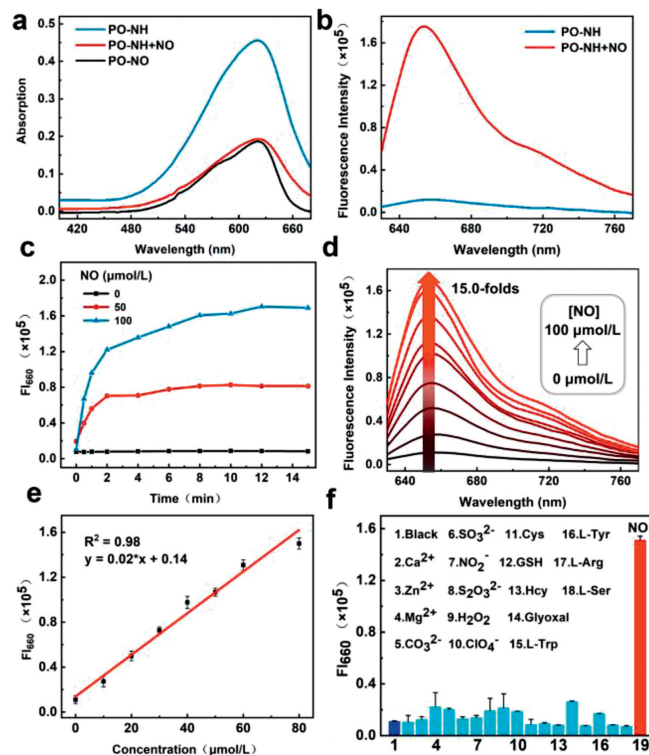


Fig. 1. (a) Absorption spectra of **PO-NO** (5 $\mu\text{mol/L}$) and **PO-NH** (5 $\mu\text{mol/L}$) after reaction with NO (100 $\mu\text{mol/L}$) for 30 min. (b) Fluorescence emission of **PO-NH** (5 $\mu\text{mol/L}$) after reaction with NO (100 $\mu\text{mol/L}$) for 30 min. (c) Kinetic study of **PO-NH** (5 $\mu\text{mol/L}$) upon addition of NO (0, 50, 100 $\mu\text{mol/L}$). (d) Fluorescence spectra of **PO-NH** (5 $\mu\text{mol/L}$) treated with NO (0–100 $\mu\text{mol/L}$) for 30 min. (e) Linear relationship between fluorescence intensity and NO (0–80 $\mu\text{mol/L}$) concentration at 660 nm. (f) Fluorescence intensity of **PO-NH** (5 $\mu\text{mol/L}$) at 660 nm after 30 min response with different substances (200 $\mu\text{mol/L}$). Black: **PO-NH**, 2: Ca^{2+} , 3: Zn^{2+} , 4: Mg^{2+} , 5: CO_3^{2-} , 6: SO_3^{2-} , 7: NO_2^- , 8: $\text{S}_2\text{O}_3^{2-}$, 9: H_2O_2 , 10: ClO_4^- , 11: Cys, 12: GSH, 13: Hcy, 14: Glyoxal, 15: L-Trp, 16: L-Tyr, 17: L-Arg, 18: L-Ser. Data are presented as the mean value, and the error bars represented the standard deviation (SD) from the mean value ($n = 3$).

lationship for the detection of NO ($R^2 = 0.98$, Fig. 1e). Moreover, the reaction kinetics of **PO-NH** at different concentrations of NO (0, 50, 100 $\mu\text{mol/L}$) was studied. As shown in Fig. 1c, after the addition of NO, the fluorescent intensity of **PO-NH** at 660 nm was nearly stable within 8 min (Fig. 1c, Fig. S2 in Supporting information), which provides a guarantee for real-time detection. In addition, the corresponding detection limits is calculated ($k = 3$) to be 0.651 $\mu\text{mol/L}$ for NO. The complexity of the biological environment always causes difficulties for the probe application, so the specificity of the probe is the basis for *in vivo* analysis. Therefore, we evaluated the selectivity of **PO-NH**. When these bio-related substances co-existed with **PO-NH** in PBS buffer, there was no significant change in fluorescent intensity. However, when NO was added, the emission peak at 660 nm was significantly enhanced, which showed excellent selectivity for NO (Fig. 1f).

Encouraged by the results *in vitro* testing, we further investigated its ability to monitor the change of NO content in cellular level. Prior to bioimaging, the cytotoxicity of **PO-NH** was assessed by cell counting kit-8 (CCK-8). We evaluated the biotoxicity of the probe in HeLa and PC12 cells, respectively. Until the probe concentration is increased to 20 $\mu\text{mol/L}$, the survival rate of both cells could reach above 80% (Fig. S5 in Supporting information). These results show that the probe itself has excellent biocompatibility. Therefore, we further explored the ability of **PO-NH** to monitor exogenous and endogenous NO in cells. HeLa cells stained by the probe showed a very weak fluorescent signal. But, when the

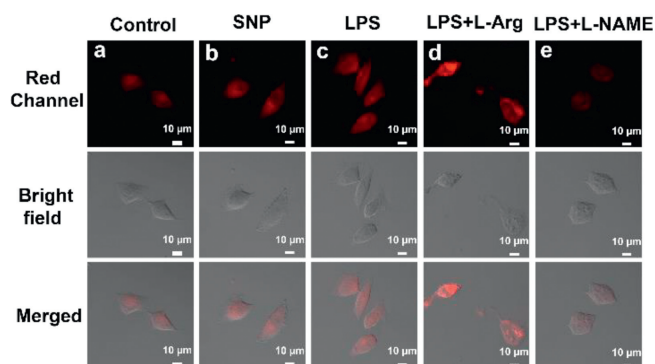


Fig. 2. Confocal imaging of extrinsic to endogenous NO level in living HeLa cells. (a) Control group: Cells and probe **PO-NH** (5 μmol/L) were incubated for 5 min. (b) SNP group: The cells were first incubated with SNP (300 μmol/L) for 1 h, followed by probe staining. (c) LPS group: The cells were incubated with LPS (20 μg/mL) for 12 h, followed by probe staining. (d) The cells were incubated with LPS (20 μg/mL) and L-Arg (5 mg/mL) for 12 h, followed by probe staining. (e) The cells were incubated with LPS (20 μg/mL) and L-NAME (0.5 mmol/L) for 12 h, followed by probe staining. Red channel: (λ_{em} = 650–720 nm, λ_{ex} = 633 nm). Scale bars: 10 μm.

cells were pretreated with sodium nitroprusside dihydrate (SNP), a widely used NO donor [38], the intracellular fluorescent signal was significantly enhanced (Fig. 2). This suggests that **PO-NH** can effectively detect exogenous NO in living cells.

Lipopolysaccharide (LPS) and L-arginine (L-Arg) are well-known NO stimulants that induce endogenous NO level to rise [39]. When the cells were pretreated with LPS or LPS + L-Arg, the cells showed significantly enhanced fluorescent signal compared with the control group (Fig. 2). At the same time, NG-nitroarginine methyl ester hydrochloride (L-NAME) as an NOS inhibitor to eliminate endogenous NO in cells [40]. Herein, we used it as a negative control group. The fluorescent intensity of cells pretreated with L-NAME decreased significantly, indicating that it effectively inhibited the production of endogenous NO (Fig. 2). Therefore, **PO-NH** can effectively detect endogenous and exogenous NO.

Rotenone is often used to establish PD model, which induces oxidative stress and leads to the loss of dopaminergic neurons [41]. As shown in Fig. 3, **PO-NH** was incubated with the cells, imaging results showed that the fluorescent intensity of PD model was significantly stronger than that of control group. This showed that NO concentration was increased by the rotenone-induced PD model group, in other words, NO in the cellular PD model was monitored by **PO-NH**.

As an optimal intracranial NO imaging probe, several requirements must be met including excellent sensitivity and selectivity for NO, NIR emission, and excellent BBB penetration capacity. Previous experiments have demonstrated the superior reactivity of **PO-NH** to NO. Therefore, to evaluate whether **PO-NH** could effec-

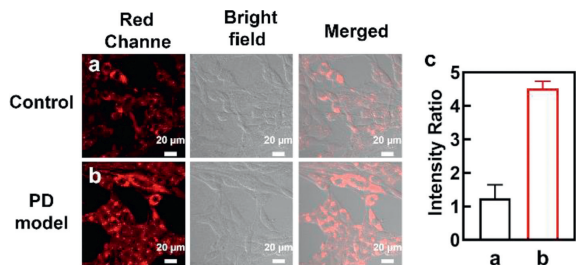


Fig. 3. Imaging of PC12 cells PD model with **PO-NH**. (a) Control group: Untreated cells were incubated with **PO-NH** (5 μmol/L, 5 min). (b) PD model: Cells treated with rotenone (1 μmol/L) for 1 h were then incubated with **PO-NH** (5 μmol/L, 5 min). (c) Average fluorescence intensity ratio between control (a) and PD model (b) groups. Data are presented as mean \pm SD (n = 3). Scale bars: 20 μm.

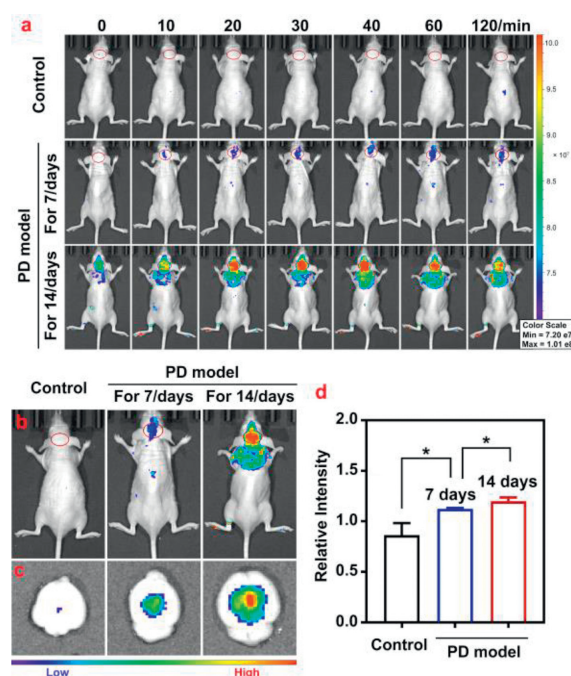


Fig. 4. *In vivo* imaging of NO in PD mice with different stages. (a) *In vivo* fluorescence imaging within 2 h in the brains of control and PD mice by injection of **PO-NH** (100 μmol/L, 150 μL) through a tail vein. (b) After injecting **PO-NH** (100 μmol/L, 150 μL) into the tail vein for 1 h, fluorescence imaging was performed on PD mice at different periods. (c) Fluorescence intensity of PD mice brain in different stages was observed by anatomical experiment. (d) Quantitative data of fluorescence intensity in brain of PD mice at different stages. Data are presented as mean \pm SD (n = 3). * P < 0.05. Red channel: λ_{em} = 700 \pm 20 nm (λ_{ex} = 640 nm).

tively cross the BBB, lipophilicity (log P , one key consideration for crossing BBB for small molecules) was estimated [42,43]. The log P value of **PO-NH** was 1.08, indicating that **PO-NH** had the potential to penetrate the BBB.

In order to study the changes of NO levels in the brain of mice at different PD stages, BALB/c-nu mice induced by methyl-4-phenyl-1,2,3,6-tetrahydropyridine (MPTP) for different days (7, 14 days) were selected as the middle and late PD models. All the animal experiments were performed by following the protocols approved by Radiation Protection Institute of Drug Safety Evaluation Center in China (Production license: SYXK (Jin) 2023–0007). BALB/c-nu mice injected with the same volume of saline were selected as the control group. As shown in Fig. 4a, after **PO-NH** (100 μmol/L 150 μL) was injected through the tail vein, the time-dependent fluorescence imaging showed different concentrations of NO in each group's mouse brains. In PD mice, the fluorescent intensity increased significantly during 0–40 min and remained stable within 40–120 min. By contrast, without obvious fluorescent signal was observed in the control group. To one's excitement, the fluorescent intensity of PD model group after 14 days of drug induction was higher than that control group and after 7 days of drug induction (Fig. 4b). After quantifying the data, we can observe this phenomenon more directly (Fig. 4d). To confirm that the probe was concentrated at the mouse brains after the tail vein was injected, we performed *in vitro* NIR imaging of the brains of anatomic PD and control group (Fig. 4c). *In vitro* imaging results showed that the level of NO in the brain increased significantly with the aggravation of PD. This further confirmed the BBB crossing ability and NO detection performance of **PO-NH**. Therefore, it is reasonable to believe that **PO-NH** can be used as a potential tool to study the involvement of NO in different stages of PD.

In summary, we have designed and synthesized a NIR probe (**PO-NH**) that can be activated by NO. **PO-NH** showed remarkable responsiveness, selectivity and high sensitivity for NO. At the cellular level, **PO-NH** is able to monitor the dynamic process of NO levels in living cells. Moreover, due to its ideal structure characteristics including its small molecular weight, log*P* value and moderate water solubility, **PO-NH** can effectively cross the BBB. This advantage enables real-time *in vivo* imaging of fluctuations in NO concentrations in the brain. Notably, facilitated by **PO-NH**, we found that with the deterioration of PD, the level of NO gradually increased in the brain of PD mice. The current study results confirmed that the variation of NO concentration in the brain is closely related to the development of PD. We envision that this work will further improve our knowledge of the diagnosis and therapy for PD.

Declaration of competing interest

The authors declare that they have no known competing financial interests or personal relationships that could have appeared to influence the work reported in this paper.

CRediT authorship contribution statement

Tao Liu: Writing – original draft. **Xuwei Han**: Formal analysis. **Xueyi Sun**: Validation. **Weijie Zhang**: Validation. **Ke Gao**: Investigation. **Runan Min**: Validation. **Yuting Tian**: Formal analysis. **Caixia Yin**: Project administration.

Acknowledgments

We thank the Program of Graduate Education and Teaching Reform of Shanxi (No. 2022YJJG302), the Applied Basic Research Programs of Shanxi (Nos. 201801D221106, 202203021221228), the Key R&D Project of Lvliang (No. 2023GXYP04), and Scientific Instrument Center of Shanxi University (No. 201512). The authors sincerely thank Suzhou Deyo Bot Advanced Materials Co., Ltd. and Professor Wentai Wang for providing support on material characterization.

Supplementary materials

Supplementary material associated with this article can be found, in the online version, at doi:10.1016/j.ccllet.2024.110170.

References

- [1] A.I. Kaplin, M. Williams, *Neurology* 69 (2007) 410.
- [2] W. Poewe, K. Seppi, C.M. Tanner, et al., *Nat. Rev. Dis. Primers* 3 (2017) 17013.
- [3] A.A. Moustafa, S. Chakravarthy, J.R. Phillips, et al., *Neurosci. Biobehav. Rev.* 68 (2016) 727–740.
- [4] J. Jankovic, *J. Neurol. Neurosurg. Psychiatry* 79 (2008) 368–376.
- [5] M.A. Hely, W.G.J. Reid, M.A. Adena, G.M. Halliday, J.G.L. Morris, *Mov. Disord.* 23 (2008) 837–844.
- [6] K.M.L. Cramb, D. BeccanoKelly, S.J. Cragg, R.Wade Martins, *Brain* 146 (2023) 3117–3132.
- [7] X.X. Wang, X.R. Hao, J. Yan, et al., *Chin. Chem. Lett.* 34 (2023) 108230.
- [8] A. MizrahiKliger, K. Ganguly, *Nat. Med.* 29 (2023) 2713–2715.
- [9] F.M. Lu, Z. Yuan, *Med. Surg.* 5 (2015) 433–447.
- [10] G. Arribarat, P. Péran, *Curr. Opin. Neurol.* 33 (2020) 222–229.
- [11] N. AbbasiGharibkandi, S.J. Hosseinimehr, *Eur. J. Med. Chem.* 166 (2019) 75–89.
- [12] A. Aliyan, N.P. Cook, A.A. Martí, *Chem. Rev.* 119 (2019) 11819–11856.
- [13] R. Qi, E. Sammler, C.P. Gonzalez-Hunt, et al., *Sci. Transl. Med.* 15 (2023) eabo1557.
- [14] P. Calabresi, G. Di-Lazzaro, G. Marino, F. Campanelli, V. Ghiglieri, *Brain* 146 (2023) 3587–3597.
- [15] C.G. Dai, J.L. Wang, Y.L. Fu, H.P. Zhou, Q.H. Song, *Anal. Chem.* 89 (2017) 10511–10519.
- [16] W. Fu, C. Yan, Z. Guo, et al., *J. Am. Chem. Soc.* 141 (2019) 3171–3177.
- [17] Y. Geng, Z. Wang, J. Zhou, et al., *Chem. Soc. Rev.* 52 (2023) 3873–3926.
- [18] H. Li, D. Kim, Q. Yao, et al., *Angew. Chem. Int. Ed.* 60 (2021) 17268–17289.
- [19] Q. Xu, Y. Zhang, M. Zhu, et al., *Chem. Sci.* 14 (2023) 4091–4101.
- [20] L. Gao, W. Wang, X. Wang, et al., *Chem. Soc. Rev.* 50 (2021) 1219–1250.
- [21] H. Kang, W. Shu, J. Yu, et al., *Anal. Chem.* 95 (2023) 6295–6302.
- [22] K. Chachlaki, V. Prevot, *Br. J. Pharmacol.* 177 (2020) 5437–5458.
- [23] H.C. Çubukçu, M. Yurtdaş, Z.E. Durak, et al., *Neurol. Sci.* 37 (2016) 1793–1798.
- [24] M.K. Tripathi, M. Kartawy, H. Amal, *Redox. Biol.* 34 (2020) 101567.
- [25] K. Solanki, S. Rajpoot, E.E. Bezonov, et al., *Peer. J.* 10 (2022) e13651.
- [26] L. Zhang, V.L. Dawson, T.M. Dawson, *Pharmacol. Ther.* 109 (2006) 33–41.
- [27] Z. Zheng, S. Gong, J. Zhang, Y. Liu, G. Feng, *Sensor. Actuat. B: Chem.* 397 (2023) 134654.
- [28] S.T. Liu, Y. Zhu, P. Wu, H. Xiong, *Anal. Chem.* 93 (2021) 4975–4983.
- [29] Y.H. Pan, X.X. Chen, L. Dong, et al., *Chin. Chem. Lett.* 32 (2021) 3895–3898.
- [30] C.J. Reinhardt, E.Y. Zhou, M.D. Jorgensen, G. Partipilo, J. Chan, *J. Am. Chem. Soc.* 140 (2018) 1011–1018.
- [31] F. Xu, Q. Wang, L. Jiang, et al., *Anal. Chem.* 94 (2022) 4072–4077.
- [32] X.X. Chen, L.Y. Niu, Q.Z. Yang, *Anal. Chem.* 93 (2021) 3922–3928.
- [33] D. Furtado, M. Björnmalm, S. Ayton, et al., *Adv. Mater.* 30 (2018) 1801362.
- [34] W. Tang, W. Fan, J. Lau, et al., *Chem. Soc. Rev.* 48 (2019) 2967–3014.
- [35] Z. Jiang, Z. Liang, Y. Cui, et al., *J. Am. Chem. Soc.* 145 (2023) 7952–7961.
- [36] L.L. Long, W.G. Liu, P. Ruan, et al., *Anal. Chem.* 94 (2022) 2803–2811.
- [37] S. Jenni, K. Renault, G. Dejoux, et al., *ChemPhotoChem* 6 (2022) e202100268.
- [38] V.K. Singh, B. Lal, *Reproduction* 153 (2017) 133–146.
- [39] D. Cheng, Y. Pan, L. Wang, et al., *J. Am. Chem. Soc.* 139 (2016) 285–292.
- [40] A. Tarrade, E. Lecarpentier, S. Gil, et al., *Placenta* 35 (2014) 254–259.
- [41] M. Ramalingam, Y.J. Huh, Y.I. Lee, *Front. Neurosci.* 13 (2019) 1028.
- [42] M. Gupta, H.J. Lee, C.J. Barden, D.F. Weaver, *J. Med. Chem.* 62 (2019) 9824–9836.
- [43] L. Shen, H.M. Liu, M. Jin, et al., *Chin. Chem. Lett.* 35 (2024) 109572.